

The Small, Secreted Immunoglobulin Protein ZIG-3 Maintains Axon Position in *Caenorhabditis elegans*

Claire Bénard,¹ Nartono Tjoe, Thomas Boulin, Janine Recio and Oliver Hobert

Department of Biochemistry and Molecular Biophysics, Howard Hughes Medical Institute, Columbia University Medical Center, New York, New York 10032

Manuscript received July 20, 2009

Accepted for publication September 5, 2009

ABSTRACT

Vertebrate and invertebrate genomes contain scores of small secreted or transmembrane proteins with two immunoglobulin (Ig) domains. Many of them are expressed in the nervous system, yet their function is not well understood. We analyze here knockout alleles of all eight members of a family of small secreted or transmembrane Ig domain proteins, encoded by the *Caenorhabditis elegans* *zig* (“zwei Ig Domänen”) genes. Most of these family members display the unusual feature of being coexpressed in a single neuron, PVT, whose axon is located along the ventral midline of *C. elegans*. One of these genes, *zig-4*, has previously been found to be required for maintaining axon position postembryonically in the ventral nerve cord of *C. elegans*. We show here that loss of *zig-3* function results in similar postdevelopmental axon maintenance defects. The maintenance function of both *zig-3* and *zig-4* serves to counteract mechanical forces that push axons around, as well as various intrinsic attractive forces between axons that cause axon displacement if *zig* genes like *zig-3* or *zig-4* are deleted. Even though *zig-3* is expressed only in a limited number of neurons, including PVT, transgenic rescue experiments show that *zig-3* can function irrespective of which cell or tissue type it is expressed in. Double mutant analysis shows that *zig-3* and *zig-4* act together to affect axon maintenance, yet they are not functionally interchangeable. Both genes also act together with other, previously described axon maintenance factors, such as the Ig domain proteins DIG-1 and SAX-7, the *C. elegans* ortholog of the human L1 protein. Our studies shed further light on the use of dedicated factors to maintain nervous system architecture and corroborate the complexity of the mechanisms involved.

NERVOUS systems display an enormous morphological complexity. They are built through the interplay of a plethora of molecular mechanisms that dictate the precise positioning of neuronal cell bodies, axons, dendrites, and synapses. After functional circuits have been established and have begun to operate, nervous systems require dedicated cells and molecules to maintain circuitry structure (BÉNARD and HOBERT 2009). Such active maintenance mechanisms were first described in some molecular and cellular detail in the nematode *Caenorhabditis elegans*. Its precisely mapped and invariantly structured nervous system allows to probe with unprecedented detail the effect of removing individual cells and genes. Genetic and cellular ablation studies have revealed that a number of diverse Ig domain proteins are required to maintain the precise positioning of axons within fascicles and cell bodies within ganglia (ZALLEN *et al.* 1999; AURELIO *et al.* 2002; BÜLOW *et al.* 2004; SASAKURA *et al.* 2005; WANG *et al.* 2005; BÉNARD *et al.* 2006; POCKOCK *et al.* 2008). Intriguingly, without these molecules nervous system

development is unaffected, yet precise neuroanatomical patterns are lost postdevelopmentally. In other words, within the nervous system, these molecules are dedicated to a role in maintaining the architectural integrity of neuronal circuitry.

Maintenance factors function at specific postembryonic stages (“critical stages”) and they serve to counter disruptive environmental factors, the most notable being mechanical forces exerted onto fascicles and ganglia via movement of the animal. When such movement is inhibited, these displacing forces are absent and consequently maintenance factors are no longer required (AURELIO *et al.* 2002; SASAKURA *et al.* 2005; BÉNARD *et al.* 2006; POCKOCK *et al.* 2008).

Maintenance factors are required for preserving two prominent structures in *C. elegans*, axons within the ventral nerve cord and neuronal cell bodies in head ganglia (BÉNARD and HOBERT 2009). The ventral nerve cord of *C. elegans* is shown schematically in Figure 1. At hatching, the first stage larva (L1 larva) contains only a few axons in the left ventral cord and numerous axons in the right ventral nerve cord. Both cords are separated by a midline composed of motor neuron cell bodies (Figure 1) and at later larval and adult stages by a hypodermal evagination called the hypodermal ridge. The loss of either one of four previously described axon

Supporting information is available online at <http://www.genetics.org/cgi/content/full/genetics.109.107441/DC1>.

¹Corresponding author: University of Massachusetts Medical School, 364 Plantation St., Worcester, MA 01605.
E-mail: Claire.Benard@umassmed.edu

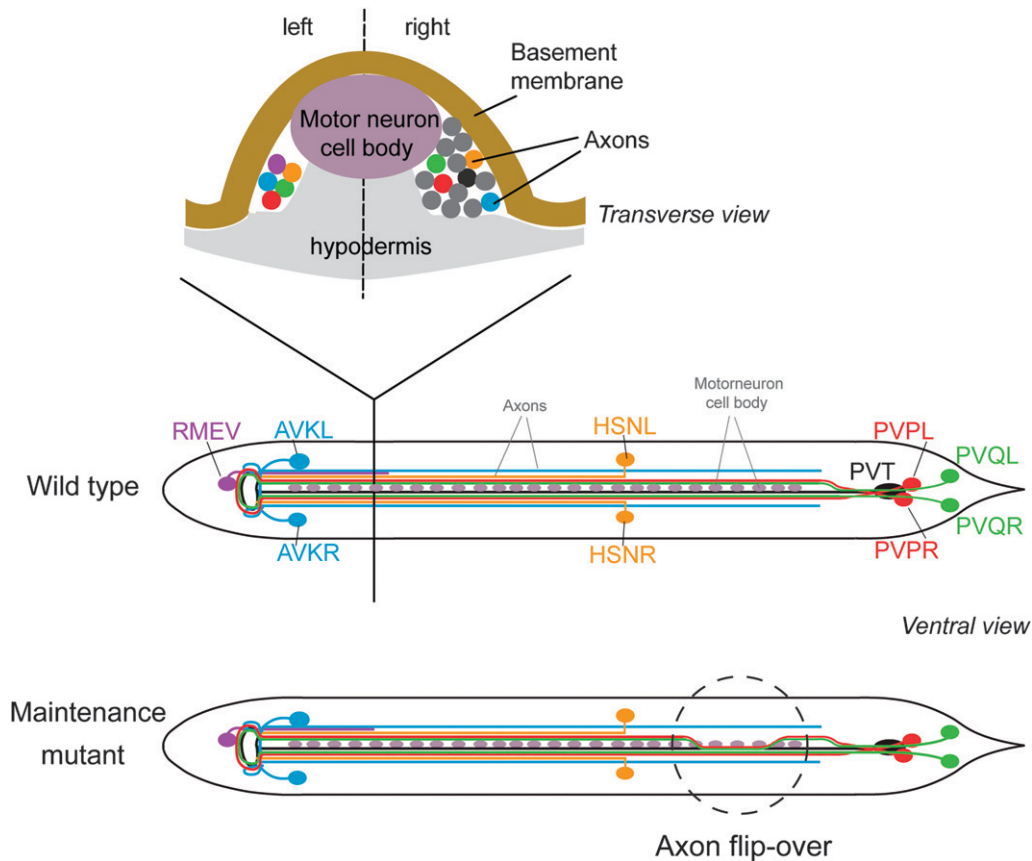


FIGURE 1.—Overview of the ventral nerve cord in *C. elegans*. Nervous system architecture of *C. elegans* has been described in detail by WHITE *et al.* (1986).

maintenance factors, *dig-1*, *sax-7* (human L1 ortholog), *egl-15* (FGF receptor ortholog), and *zig-4* results in seemingly identical phenotypes (AURELIO *et al.* 2002; BÜLOW *et al.* 2004; BÉNARD *et al.* 2006; POCKOCK *et al.* 2008): Axons develop normally in the embryo and appear normally positioned at the early L1 stage, but shortly thereafter become displaced through movement of the animal. *sax-7* appears to act autonomously within neurons (POCKOCK *et al.* 2008) and *dig-1* cell nonautonomously from muscle (BÉNARD *et al.* 2006); both factors also are required to maintain cell body position in head ganglia. In contrast, *egl-15* and *zig-4* are only required to maintain axon position in the ventral nerve cord; to fulfill this role, *egl-15* acts in the hypodermis that underlies that ventral nerve cord (BÜLOW *et al.* 2004) and *zig-4* appears to be secreted from PVT, a unilateral neuron that extends an axon along the ventral cord. PVT ablation phenocopies the loss of *zig-4* (AURELIO *et al.* 2002). How all these factors interact is at present not understood.

To better understand the maintenance of neuronal architecture, we set out to identify additional maintenance factors. The previously identified maintenance factor ZIG-4 is a member of a family of eight ZIG proteins, which are all defined by their common domain architecture. Each protein is composed of two Ig domains (hence the name “Zwei Ig Domänen”) and is predicted to be either secreted (ZIG-2–ZIG-8) or cell

surface associated on the basis of the presence of a transmembrane domain (ZIG-1) (Figure 2A). On the primary sequence level, *C. elegans* ZIG proteins are diverse (Figure 2B) and apparently fast evolving, as evidenced in the distinct complement of ZIG proteins apparent in the related nematodes *C. briggsae* and *C. remanei* (www.wormbase.org). Fly and vertebrate genomes also contain scores of small secreted or transmembrane two-Ig domain proteins, which, however, bear little primary sequence similarity to ZIG proteins (ROUGON and HOBERT 2003).

Aside from *zig-4*, no other *zig* gene has previously been functionally characterized. In this article we address the question of whether other *zig* family members may, like *zig-4*, also be involved in maintaining nervous system structure. This seemed a particularly attractive possibility as many family members are expressed by the same neuron in the ventral cord, PVT, which we found to be required for maintaining fascicle structure (AURELIO *et al.* 2002). Moreover, since *zig-4* mutants affect the maintenance of only a subset of axons in the ventral nerve cord, the question arose whether other *zig* genes affect other axons. Lastly, other maintenance factors, such as *dig-1* or *sax-7* affect cell body position, prompting the question of whether other ZIG proteins affect the maintenance of cell body position as well. To address these questions we undertook a systematic functional analysis of all *zig* family members using genetic

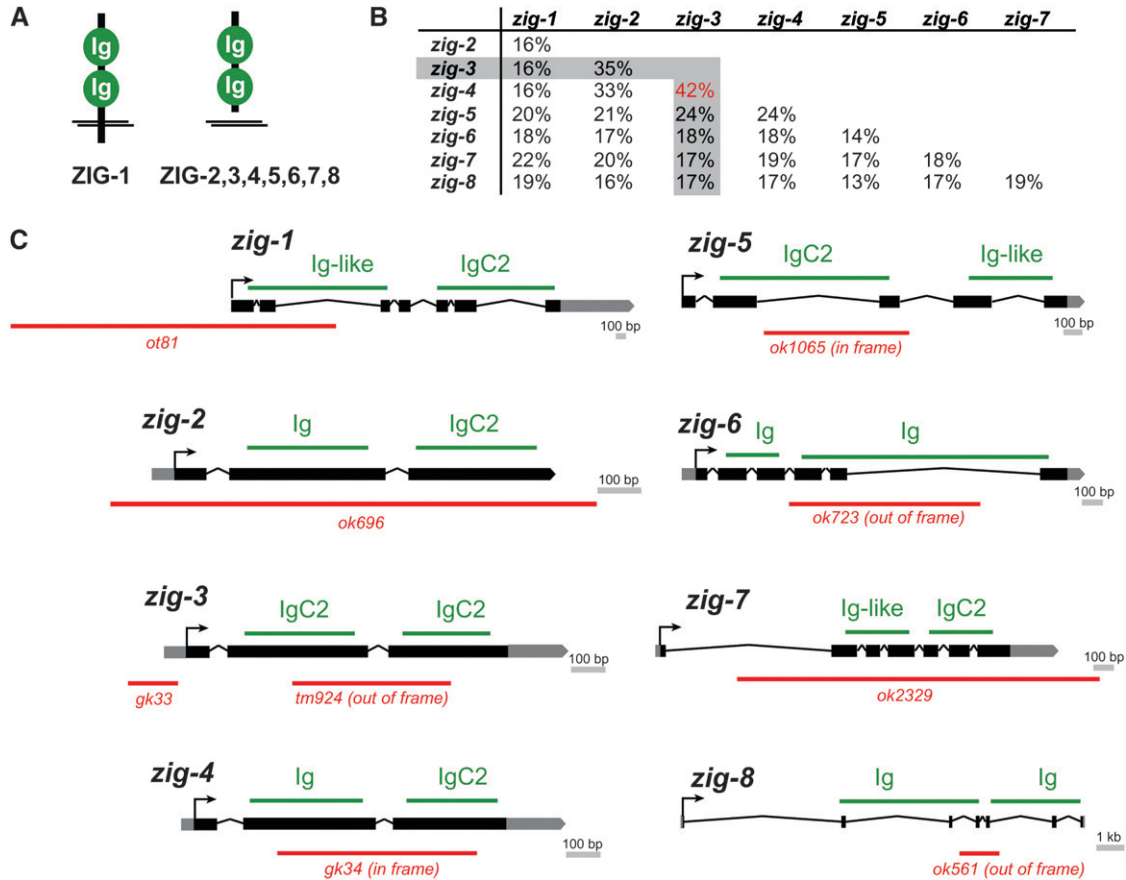


FIGURE 2.—*zig* genes, proteins and mutant alleles. (A) Schematic structure of ZIG proteins. (B) Sequence comparison of ZIG proteins. Percent identity was calculated from alignment done with T-coffee (NOTREDAME *et al.* 2000). (C) *zig* mutant alleles. The type of Ig domains are indicated as identified by SMART (<http://smart.embl-heidelberg.de/>).

deletion alleles. We report the result of these studies in this article.

MATERIALS AND METHODS

Strains: Strains were maintained as described (BRENNER 1974). A list of all strains used in this study is provided in the supporting information, File S1.

All deletion alleles were generated by the *C. elegans* knockout consortia through PCR screening of mutagen-induced deletion libraries, with the exception of *zig-1(ot81)*. The *zig-1(ot81)* deletion allele was generated by spontaneous imprecise excision of a *Tc1* transposable element from the strain *cxTi6127; mut-7(pk204) dpy-18(e364)* provided by Laurent Segalat. This strain carries a *Tc1* transposon insertion at position 3301 in the cosmid K10C3. In brief, 10 adult worms were placed on 150 plates and grown at 20° until food was exhausted. Half of the worms were then collected from each plate, lysed, and screened for deletion products by PCR. Positive plates were chunked in four parts and retested by PCR. Finally, single worms were picked from positive plates to isolate a homozygous deletion mutant. Sequencing of the *zig-1(ot81)* breakpoints revealed a 2281-bp deletion from position 3282–5563 in K10C3, which deletes the first two exons, the entire first intron, and part of the second intron of *zig-1*. All alleles were outcrossed with N2 at least three times.

Genotyping of *zig* gene alleles throughout various genetic crosses was carried out by PCR, as their deletion results in no

obvious morphological or behavioral phenotypes. PCR was done on genomic DNA preparations, generated by lysing mixed population of worms grown on agar plates using a standard protocol (FAY and BENDER 2008). Primers used for PCR are listed in Table S1.

The genes *zig-3* and *zig-4* map only 0.06 cM apart on LGX (<5 kb apart). To minimize the effort of screening by PCR for a recombinant between these two genes, we used the genetic markers *lon-2(e678)* and *unc-115(mn481)* flanking *zig-3* and *zig-4*. On LGX, *lon-2* is located at –6.7 cM, *zig-4* at –1.00 cM, *zig-3* at –0.94 cM, and *unc-115* at 1.88 cM. We first generated the two starting strains, *lon-2(e678) zig-4(gk34)* and *zig-3(tm924) unc-115(mn481)*, by genetic recombination from heterozygous worms of genotypes *lon-2 unc-18/zip-4* and *dpy-6 unc-115/zip-3*, respectively. We then crossed *lon-2 zig-4/00* males into *zig-3 unc-115* hermaphrodites to obtain heterozygous hermaphrodites *lon-2 zig-4/zip-3 unc-115*. From these heterozygous F₁ worms, we picked a total of 800 Lon or Unc F₂ worms. Two hundred eighty-six of these Lon or Unc F₂ are expected to carry a recombinant chromosome of the type *lon-2 unc-115*, among which only 2 would be *lon-2 zig-4 zip-3 unc-115*, brought about by a recombination event taking place between *zig-3* and *zig-4*. We homozygosed *lon-2 unc-115* chromosomes by singling F₃ worms that were Lon and Unc. We lysed worms and analyzed by PCR for the presence of both *zig-3* and *zig-4* mutant and wild-type alleles to detect recombinants occurring between these two genes. We obtained one recombinant *lon-2 zig-4 zip-3 unc-115*. We then proceeded to get a *zig-4 zig-3* strain devoid of the intermediate markers *lon-2* and *unc-115*. We first removed

TABLE 1
Axon anatomy transgenic markers

Transgene name	Reporter construct	Cell(s) labeled	Reference
<i>oyIs14</i>	<i>sra-6::gfp</i>	PVQ, ASH, ASI	SARAFI-REINACH <i>et al.</i> (2001)
<i>hdIs26, hdIs29</i>	<i>sra-6::DsRed2</i>	PVQ, ASH, ASI PVP, and other	HUTTER (2003)
	<i>odr-2::cfp</i>	head and VNC neurons	
<i>oxIs12</i>	<i>unc-47::gfp</i>	RMEV and all other GABAergic neurons	McINTIRE <i>et al.</i> (1997)
<i>juIs8</i>	<i>unc-25::gfp</i>	RMEV and all other GABAergic neurons	JIN <i>et al.</i> (1999)
<i>zdIs13</i>	<i>tph-1::gfp</i>	HSN, ADF, NSM	CLARK and CHIU (2003)
<i>bwIs2</i>	<i>flp-1::gfp</i>	AVK only	MUCH <i>et al.</i> (2000)
<i>otIs173</i>	<i>F25B3.3::DsRed2</i>	Panneuronal	This work

unc-115 by picking Lon-non-Unc recombinant F₂ worms from heterozygous F₁ *lon-2 zig-4 zig-3 unc-115/+*. We homozygosed *lon-non-unc* chromosomes by singling Lon F₃ worms. We lysed and analyzed them by PCR to select those retaining *zig-4 zig-3*. We next removed the marker *lon-2* by picking non-Lon F₂ worms from heterozygous F₁ hermaphrodites of the genotype *lon-2 zig-4 zig-3/oxIs12* generated by crossing *oxIs12/0* males into *lon-2 zig-4 zig-3*. *oxIs12* is a dominant transgene integrated at ~2 cM of LGX that drives *gfp* in GABAergic neurons. We selected F₃ broods with 75% *oxIs12* and no Lon worms. We next homozygosed the new *zig-4 zig-3* chromosome, devoid of *lon-2*, by selecting for non-*oxIs12* worms. We confirmed by PCR the homozygous presence of *zig-3(tm924)* and *zig-4(gk34)*.

Transgenes: Transgenes generated for rescue of mutant phenotypes are listed in File S1, with concentration of injected DNA indicated. Reporter transgenes to score neuroanatomy are listed in Table 1. They were crossed with *zig* deletion alleles and the resulting strains genotyped for the presence of the *zig* deletion alleles by PCR (Table S1). One panneuronal reporter transgene, *otIs173*, was specifically created for this study. pCB101=F25B3.3::DsRed2 was generated by cloning a *Bam*HI–*Apa*I fragment containing DsRed2 under the F25B3.3 promoter. pCB101 was injected at 50 ng/μl along with *ttx-3::gfp* at 75 ng/μl. An extrachromosomal array was integrated by gamma irradiation, by conventional protocols, yielding *otIs173*. The strain bearing *otIs173* was outcrossed 10 times. *otIs173* maps to LGIII. Another reporter transgene, *zig-3 short prom::gfp*, was generated by PCR fusion (HOBERT 2002) (PCR primers see “DNA constructs” in File S1).

DNA constructs: DNA constructs were generated by standard cloning procedures or by PCR fusion (HOBERT 2002). A list of all constructs and primer sequences can be found in File S1.

Scoring of neuroanatomy: Axon and cell body position were scored with reporter transgenes listed in Table 1. Unless otherwise indicated, animals were grown at 20° and scored using a Zeiss Axioplan 2 microscope. Axons of the ventral nerve cord were scored in freshly hatched L1 larvae as well as in young adults. To obtain freshly hatched L1 larvae, embryos were picked and allowed to hatch and develop no longer than 30 min posthatching. Young adults that have just molted from L4, have a slightly protruding vulva and no embryos in their uteri. Cell body position was examined in 3- to 5-day-old adults. All phenotypes were scored as percentage of animals defective and results are shown with error bars representing the standard error of proportion. Statistical significance was calculated using the z-test to compare the proportion of abnormal animals of two genotypes. When using the same control for multiple comparisons, the *P*-value was multiplied by the total number of comparisons.

Laser ablation: Laser ablations were performed as previously described (BARGMANN and AVERY 1995) using a Photonics dye laser (LSI VSL-337) attached to a Zeiss Axioplan 2 microscope equipped with Nomarski, and fluorescence optics were used for microscopy. Freshly hatched L1 worms were mounted in a drop of 10 μM sodium azide solution on a 5% agarose pad, sealed between a cover slip, and observed directly using Nomarski and fluorescence microscopy to identify the targeted cells. We used the *otEx2419 gcy-1::gfp* array (ORTIZ *et al.* 2006) to visualize and ablate PVT in wild-type and *zig-4 zig-3* double mutant background. For ablation of PVQL, PVQR, PVPL, and PVPR, reporter strains *oyIs14* and *hdIs26* were used, respectively. Cells were irradiated for ~3 sec in the nucleus. Increased cytoplasmic movements were often observed and in many cases the nucleus was observed to break down. Animals were recovered promptly and allowed to develop to the young adult stage at 20°, when their neuroanatomy was examined. Successful ablation of the neuron was assessed by the absence of *gfp* fluorescence at the adult stage.

RESULTS

Analysis of *zig* gene knockout alleles: Of the eight *zig* genes only one, *zig-4*, was previously analyzed through gene deletion analysis (AURELIO *et al.* 2002). Through generating deletion alleles by either transposon mobilization (*zig-1*) or deletion library screening, conducted by the *C. elegans* knockout consortia (*zig-2, -3, -5, -6, -7, and -8*), we have obtained knockout alleles for each of the so far uncharacterized, seven remaining *zig* genes in *C. elegans*. Each allele is a predicted molecular null allele (Figure 2C) and none affects viability or produces any other readily visible morphological or behavioral phenotype. Given the *zig-4* precedent and the expression of at least six of the eight *zig* genes in the PVT neuron of the ventral nerve cord (AURELIO *et al.* 2002), we analyzed ventral nerve cord architecture in all *zig* mutant animals. In addition, we also examined the correct position of neuron soma; correct maintenance of soma position is controlled by other previously identified maintenance factors (ZALLEN *et al.* 1999; SASAKURA *et al.* 2005; BÉNARD *et al.* 2006). This neuroanatomical analysis was conducted by crossing a series of chromosomally integrated *gfp* reporters that allow the visualization of individual neuron types in all *zig* mutant backgrounds (Table 1). No defects were observed for any *zig* mutants in head neuron

TABLE 2
Phenotypes of *zig* mutants

Genotype	% animals with axon flip-over defects of the following neuron classes				
	PVQ	PVP	RMEV	HSN	AVK
Wild type	7%	6.0% <i>n</i> = 285 ^a	1% <i>n</i> = 118 ^c	4.7%	1%
<i>zig-1(ot81)</i>	<i>n</i> > 400	7.9% <i>n</i> = 178 ^b	1% <i>n</i> = 71 ^d	<i>n</i> = 169	<i>n</i> = 120
<i>zig-2(ok696)</i>	8%	4.9%	0%	3.2%	2.3%
	<i>n</i> = 177	<i>n</i> = 122 ^a	<i>n</i> = 86 ^c	<i>n</i> = 126	<i>n</i> = 87
<i>zig-3(tm924)</i>	8%	4%	1%	1.8%	0%
	<i>n</i> = 187	<i>n</i> = 85 ^a	<i>n</i> = 78 ^c	<i>n</i> = 112	<i>n</i> = 104
<i>zig-4(gk34)</i>	26%	20%	3.3%	0%	1%
	<i>n</i> = 201	<i>n</i> = 160 ^a	<i>n</i> = 120 ^d	<i>n</i> = 130	<i>n</i> = 196
<i>zig-4(gk34) zig-3(tm924)</i>	24%	22%	1.6%	3.8%	1%
	<i>n</i> = 189	<i>n</i> = 144 ^a	<i>n</i> = 122 ^d	<i>n</i> = 131	<i>n</i> = 105
<i>zig-4(gk34) zig-3(tm924)</i>	26%	24.6%	4.7%	10%	0%
	<i>n</i> = 299	<i>n</i> = 240 ^a	<i>n</i> = 129 ^d	<i>n</i> = 248	<i>n</i> = 85
<i>zig-5(ok1065)</i>	9%	4.4%	0%	6.3%	0%
	<i>n</i> = 194	<i>n</i> = 90 ^b	<i>n</i> = 96 ^c	<i>n</i> = 175	<i>n</i> = 93
<i>zig-6(ok273)</i>	9%	5.5%	2.6%	7%	0%
	<i>n</i> = 166	<i>n</i> = 127 ^a	<i>n</i> = 115 ^d	<i>n</i> = 116	<i>n</i> = 106
<i>zig-7(ok2329)</i>	5%	9.2%	0%	4.2%	0%
	<i>n</i> = 100	<i>n</i> = 130 ^a	<i>n</i> = 94 ^c	<i>n</i> = 118	<i>n</i> = 100
<i>zig-8(ok561)</i>	9%	11%	0%	6.5%	0%
	<i>n</i> = 193	<i>n</i> = 168 ^a	<i>n</i> = 85 ^c	<i>n</i> = 138	<i>n</i> = 70

Defects that are statistically different ($P < 0.05$) from wild type are in boldface type. Transgenes used to visualize axon anatomy: PVQ, *oyIs14*; PVP, *hdIs26^a* or *hdIs29^a*; RMEV, *oxIs12^a* or *juIs8^d*; HSN, *zdlIs13*; AVK, *bulIs2*. See Table 1 for more information on these transgenes.

position (data not shown), yet we found that *zig-3* mutants, but no other single *zig* mutants, display position defects of individual and specific sets of axons in the ventral nerve cord (Table 2; Figure 3). Two different *zig-3* alleles display similar defects and defects can be rescued by reintroducing wild-type copies of the *zig-3* genomic locus (Figure 4).

The axonal defects in *zig-3* mutants are postdevelopmental in nature, as they are not observed in freshly hatched larvae (examined at <30-min posthatching, Figure 3). That is to say, axons that have migrated along the ventral nerve cord during embryogenesis appear normal at the early L1 stage, but during later larval stages become displaced across the ventral midline. This displacement results from mechanical stress as it can be suppressed through immobilizing worms either pharmacologically or through incapacitating locomotion genetically (Figure 3). We conclude that the normal function of *zig-3* is to prevent locomotion-induced axon displacement to occur.

Genetic interactions of *zig-3*: The *zig-3* mutant defects are very similar to those seen in *zig-4* mutants, in terms of appearance, penetrance, and cellular specificity (Table 2). We generated a double null mutant of *zig-3* and *zig-4* and find that those double mutant animals display similar phenotypes compared to those observed in the respective single null mutants (Figure 5A). The failure to enhance null mutant phenotypes usually is an indication of two genes acting in the same genetic pathway.

In the case of *ZIG-3* and *ZIG-4*, acting in a similar pathway may mean that both proteins may act together in a complex, as many other Ig proteins do (BARCLAY *et al.* 1997). We note that failure to enhance each other's null phenotype is not due to a "ceiling effect," as other mutant combinations of maintenance factors display much stronger phenotypes (C. BÉNARD and O. HOBERT, unpublished data).

The *zig-3* single mutant, the *zig-4* single mutant, and a *zig-4 zig-3* double mutant also do not enhance the VNC axon flip-over phenotype of other axon maintenance factors, namely *dig-1*, *sax-7*, and *egl-15* (Figure 5B). This indicates that all these genes may act in one common pathway.

A regulatory allele of *zig-3* affects a neuronal cis-regulatory sequence: Where does *zig-3* act to affect axon maintenance? We had previously reported that 4.4 kb of 5' upstream regulatory sequences of the *zig-3* locus drive *gfp* reporter gene expression in PVT and a few other neurons and that ablation of PVT displays axon maintenance defects similar to those that we now observe for *zig-3* (AURELIO *et al.* 2002). One of the two *zig-3* alleles, *gk33*, is a regulatory allele that further bolsters the hypothesis of a neuronal focus of action of *zig-3*. *gk33* animals carry a 109-bp deletion that does not affect the protein-coding part of *zig-3* but deletes sequences from 129 to 20 bp upstream of the predicted start codon of *zig-3* (Figure 2). A genomic fragment of the *zig-3* locus, termed "*zig-3 short promoter*," which contains exons,

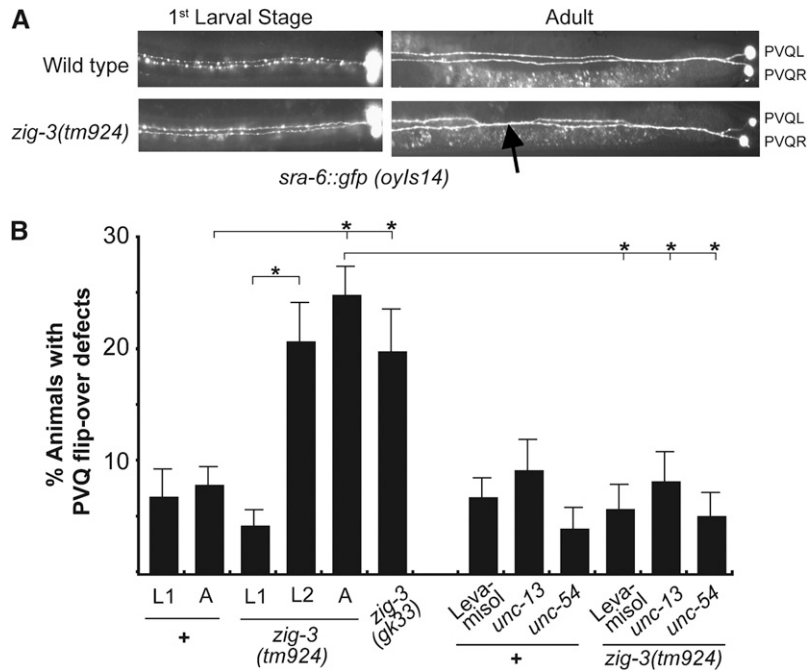


FIGURE 3.—*zig-3* mutant phenotype. (A) PVQ flip-over defects observed with the *oyIs14* reporter transgene. Most (>90%) of all axon flip-over defects observed in *zig-3* (or *zig-4*) mutant animals occur in the posterior half of the animal. (B) Quantification of *zig-3* mutant defects at different developmental stages and under different experimental conditions. Proportions of different animal populations were compared using the χ -test. * $P < 0.05$.

introns, the 3'-UTR, and those 5' upstream sequences deleted in *gk33* (plus a few dozen nucleotides) rescues the *zig-3* mutant phenotype (Figure 4). Removal of these 5' sequences from this rescuing construct abolishes rescuing activity (Figure 4) (*zig-3 promoterless*). When fused to *gfp*, the short 5' promoter shows expression in a small number of cells with the only neuron in the ventral nerve cord being PVT (Figure 4).

***zig-3* gene activity can be ectopically provided from several different cell types but normally appears to be provided by PVT:** Consistent with a focus of action of *zig-3* in PVT, we find that expression of *zig-3* under control of the *gcy-1* promoter, which is active in PVT, the gut, and a few head neurons (ORTIZ *et al.* 2006), also rescues the *zig-3* mutant phenotype (Figure 4). If we tag the *zig-3* locus with a transmembrane domain from the *pat-3* gene, and express it under control of the *gcy-1* promoter, rescuing ability is abolished, suggesting that *zig-3* must be secreted to exert its function (Figure 4).

Secreted *zig-3* can function from several distinct but not all cellular sources. If we express *zig-3* under control of the *myo-3* promoter, which is exclusively active in body wall muscle cells that abut the ventral nerve cord (OKKEMA *et al.* 1993), we observe full rescue of the mutant phenotype (Figure 4). *zig-4* expressed under control of the *myo-3* promoter can also rescue the *zig-4* mutant phenotype (Figure 4). The rescuing activity is abolished, however, when we append a transmembrane domain to the *myo-3*-driven *zig-3* gene, pointing to the need for ZIG-3 to be secreted and diffusible (Figure 4).

Expression under the control of a promoter that is active in all neurons (*unc-14*) (OGURA *et al.* 1997) and under a promoter that is active exclusively in hypodermal cells that underlie the ventral nerve cord (*dpy-7*)

(GILLEARD *et al.* 1997) also rescues the mutant phenotype (Figure 4). In contrast, *zig-3* expression under the control of the *sra-6* promoter, which is active only in the PVQ neurons in the ventral nerve cord, does not rescue the mutant phenotype (Figure 4); this is somewhat surprising and may relate to aberrant expression levels provided by this promoter or by the inability of the *sra-6* expressing cells to secrete functional ZIG-3. We conclude that as long as *zig-3* is secreted it can be supplied from different, but not necessarily all cell types. Similarly, *zig-4* can also function when heterologously supplied from distinct cell types (AURELIO *et al.* 2002).

Several additional lines of evidence besides PVT expression and heterologous rescue with the *gcy-1* promoter point to a focus of action of *zig-3*, and also of *zig-4*, in PVT. Previous laser ablation studies (AURELIO *et al.* 2002), which we recapitulate here (Figure 6C), show that postembryonic (early L1 stage) ablation of PVT phenocopies the axon maintenance defects observed in *zig-3* and *zig-4* mutant animals. If *zig-3* and *zig-4* acted from cells other than PVT, then the defects observed upon PVT ablation should be additive to those seen in *zig-3 zig-4* double mutants; if they act from PVT, the defects should not be any more severe. We find that the frequency of the flip-over defects observed upon postembryonic PVT ablation are not any more severe if done in a *zig-4 zig-3* double mutant background, consistent with PVT being the normal source of *zig-3* and *zig-4* (Figure 6C).

PVT also has *zig-3/zig-4*-independent roles: The data described above suggests that PVT provides *zig-3* and *zig-4* function. Is this the only way in which PVT affects axon maintenance? If so, then PVT would be superfluous if we provided *zig-3* and *zig-4* from heterologous cells. We

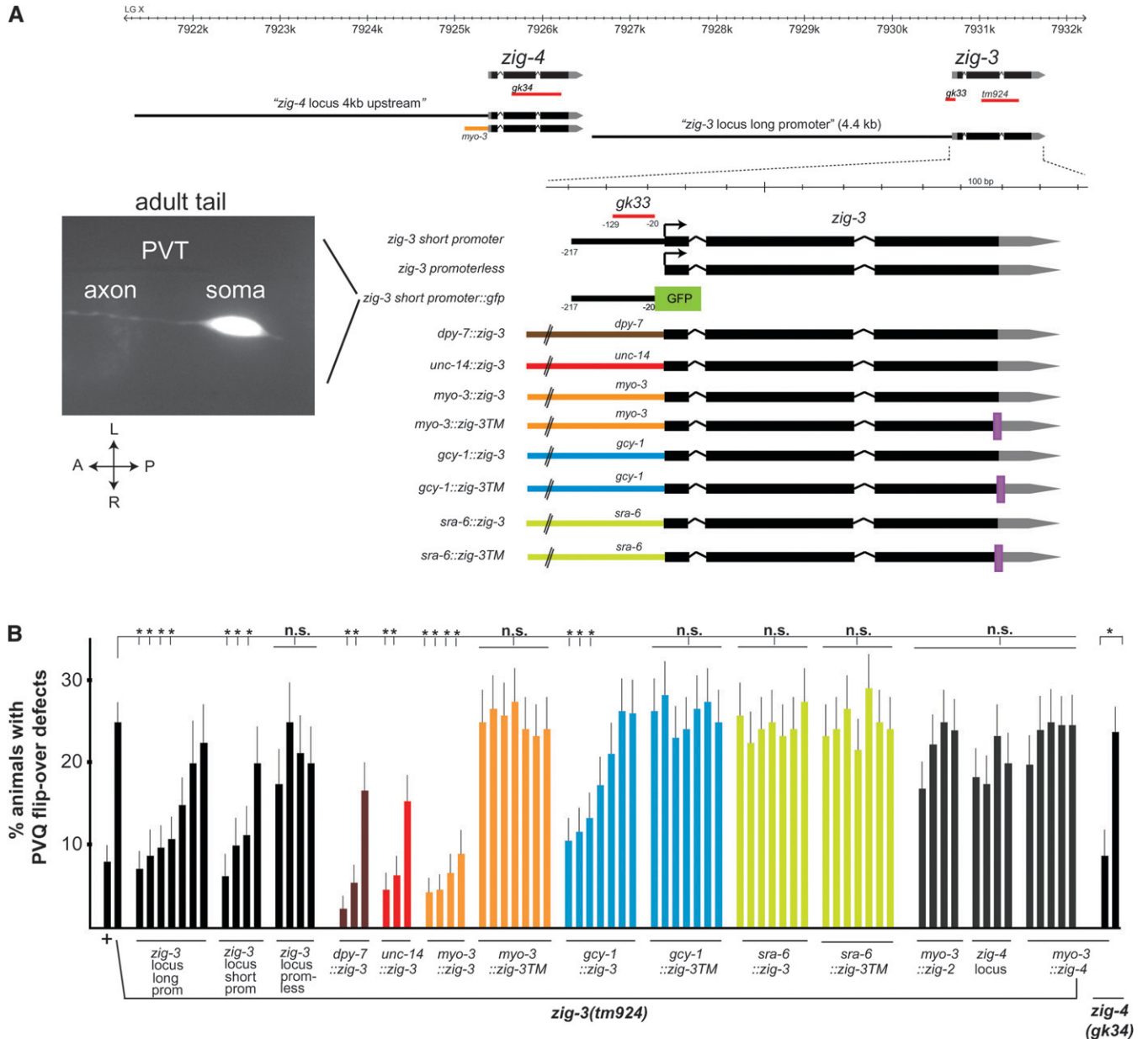


FIGURE 4.—Expression and focus of action of *zig-3*. (A) *zig-3* and *zig-4* genomic locus and constructs used to test for *zig-3* and *zig-4* rescuing activity and reporter gene analysis. Two independent transgenic lines showed the same *gfp* expression pattern. A young adult animal is shown. (B) Quantification of rescue data. Note that we have previously shown that overexpression of *zig-4*, using again the *myo-3* promoter, causes PVQ axon outgrowth defects (AURELIO *et al.* 2003). In the experiments shown here *myo-3::zig-4* was injected at lower concentration, which did not result in axon outgrowth defects. One of the *myo-3::zig-4* lines generated in the *zig-3(tm924)* background was transferred into *zig-4(gk34)* to verify its rescuing ability of the *zig-4* mutant defects. Proportions of different animal populations were compared using the *z*-test. * $P < 0.05$; NS: $P > 0.05$.

tested this in the following manner: As we described above, *zig-3* and *zig-4* gene function can be provided using the heterologous *myo-3* promoter. We corroborated that this is the case in a *zig-4 zig-3* double mutant; a transgenic array that contains both *myo-3::zig-3* and *myo-3::zig-4* can indeed rescue the *zig-4 zig-3* double mutant phenotype (Figure 6C). In those animals, *zig-3* and *zig-4* are therefore not provided from their normal cellular source (PVT) but from an ectopic source, resulting in phenotypically wild-type animals. When we ablate PVT

in those transgenic animals, we observe axon maintenance defects again (Figure 6C). This indicates that PVT does more than just providing *zig-3* and *zig-4* function. Indeed we have found that a simultaneous deletion of two other PVT-expressed and apparently redundantly acting *zig* genes also results in axon maintenance defects (C. BÉNARD and O. HOBERT, unpublished data), suggesting that PVT does provide multiple *zig* genes that act nonredundantly to control axon maintenance at the midline.

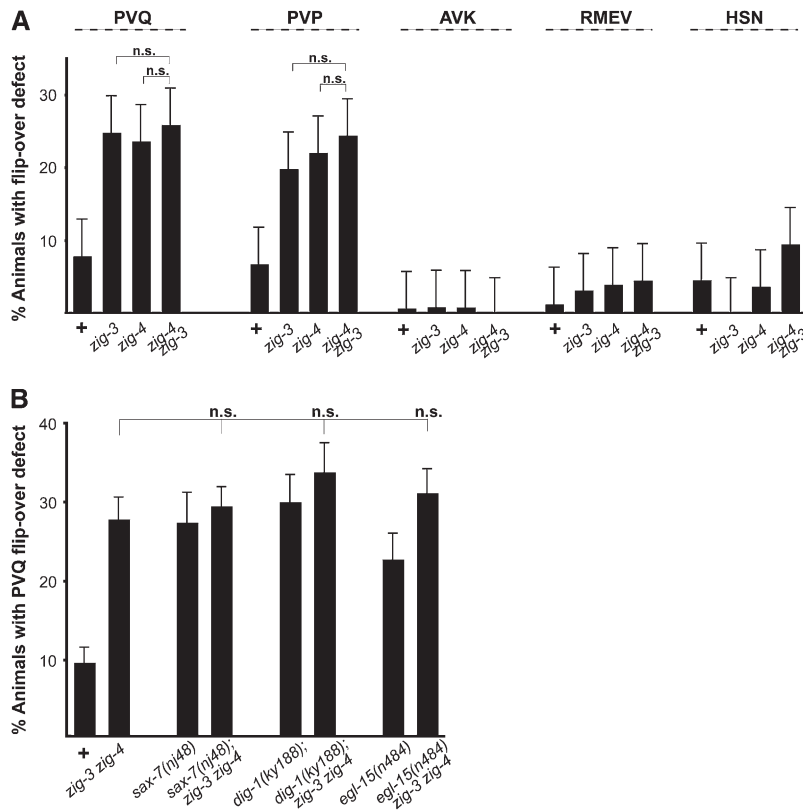


FIGURE 5.—Genetic interaction data. Genetic interaction tests of *zig-3(tm924)*, *zig-4(gk34)* and other maintenance mutants. “+” = wild-type strain, “*zig-3 zig-4*” = *zig-3(tm924) zig-4(gk34)*. See Table 1 for reporters used. All animals were scored as young adults. Proportions of different animal populations were compared using the *z*-test. NS: $P > 0.05$.

***zig* gene action is highly sequence specific:** Even though all ZIG proteins share a two-Ig domain architecture, they are very diverse at the primary sequence level, with some ZIG proteins displaying as little as 13% primary sequence identity (Figure 2). In relative terms, ZIG-3 and ZIG-4 are the most closely related ZIG proteins, not only by primary sequence (42% identical), but also by conserved intron/exon structure and chromosomal location. The two genes directly neighbor one another (Figure 4A). *zig-3* and *zig-4* therefore likely arose by local duplication that not only duplicated protein-coding sequences but also *cis*-regulatory control regions as the 5' regulatory region of each gene drives expression in PVT independently (AURELIO *et al.* 2002). In spite of these similarities, a loss of either *zig-3* or *zig-4* results in a similar mutant phenotype, not further enhanced in the double mutant. This already suggests strongly that the two genes do not act in a redundant manner. To test for gene dosage effects, we asked whether the *zig-3* mutant phenotype can be rescued by overexpressing the *zig-4*. Multicopy transgenic arrays show that this is not the case (Figure 4B). Moreover, using the *myo-3* driver, we find that only *myo-3::zig-3*, but not *myo-3::zig-4*, can rescue the *zig-3* mutant phenotype. Similarly, the *zig-2* gene, which is the second closest homolog to *zig-3* (35% primary sequence identity; Figure 2B), is also not able to rescue the *zig-3* mutant phenotype when driven under control of the *myo-3* promoter (Figure 4B).

Mechanistic aspects of the axon flip-over defect: We examined the axon flip-over defect observed in *zig-3*, as

well as in other axon maintenance mutants in more detail, with the specific goal of defining whether axons flip into the opposite fascicle of the cord or whether they stray off into more intermediate midline locations. In previous reports on axon maintenance defects (AURELIO *et al.* 2002; BÉNARD *et al.* 2006; POCKOCK *et al.* 2008), we had only scored axon flip-over defects if the left and right axons made contact with one another (as observed on the light microscopy level), leaving the possibility that more subtle mispositioning defects, in which only one axon moved onto the midline (rather than into the opposite fascicle), were not reported. Moreover, we had previously surmised that axon flip-over defects in *zig-4* show no directionality in terms of whether an axon crosses from the left to the right fascicle or vice versa (AURELIO *et al.* 2002), but without more fine-grained anatomical resolution, this conclusion was only tentative. To analyze these issues in more detail, we constructed and used a panneuronal *rff* marker transgene (*otIs173*) to unambiguously distinguish the right from the left fascicle, thereby generating a clear reference point. Animals in which the entire left and right fascicles are labeled in red and the PVQ axons are specifically labeled in green reveal that PVQ axon flip-overs observed in various maintenance factor mutant backgrounds are all-or-nothing defects (Figure 6A). No intermediate positions of flipped axons are observed. Curiously, we noted that it is exclusively the axons of the less populated left fascicle that flip over the midline (*i.e.*, PVQL) but never from the much

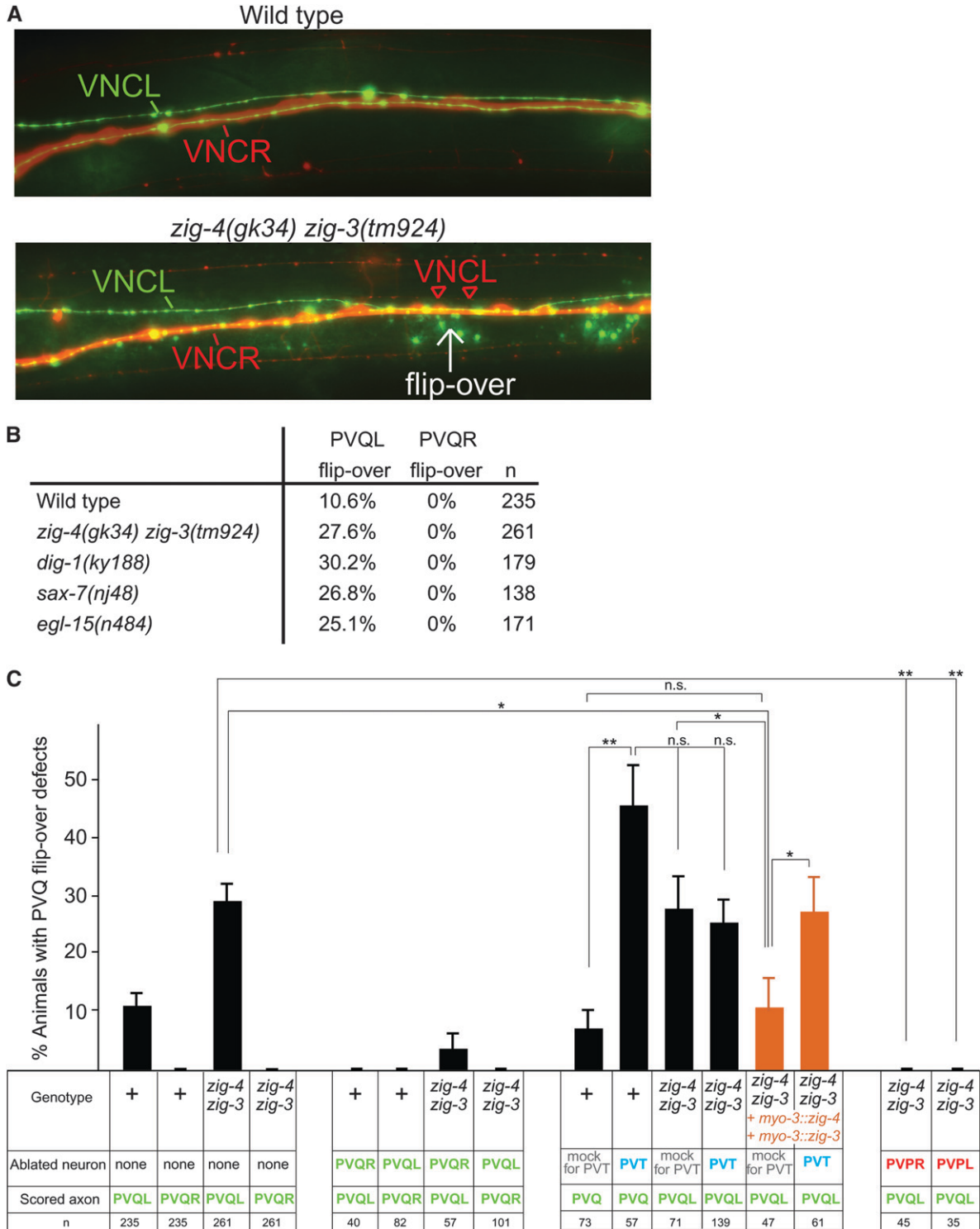


FIGURE 6.—Cellular analysis of axon midline flip-over defects. (A) Midline flip-overs are all-or-none defects as assessed by co-labeling the entire left and right ventral nerve cord fascicle with a panneuronal *rfp* marker (*otIs173*) and the PVQ neurons with a *gfp* marker (*oyIs14*). Young adult animals are shown. (B) PVQ axon flip-overs (scored in young adults with the *oyIs14* and *otIs173* transgenes) always occur from the left into the right fascicle, as scored in different maintenance factor mutant backgrounds. This also holds for the background level of flip-over in a wild-type genetic background. (C) Laser ablation data. “+” = wild-type strain; “*zig-4 zig-3*” = *zig-3(tm924) zig-4(gk34)*. For the PVT ablation experiments, a *gcy-1::gfp* transgene was placed into the genetic background to visualize PVT. PVQ axons and soma were visualized with *oyIs14* and PVP axons and soma with *hdIs26*. Proportions of different animal populations were compared using the *z*-test. **P* < 0.05; ***P* < 0.01; and NS: *P* > 0.05.

thicker right fascicle into the left fascicle (Figure 6, A and B).

As a flipped-over axon always appears to make contact with its contralateral analog, at least on the light microscopy level, we asked whether PVQR is required for the manifestation of the PVQL flip-over defect observed in *zig* mutants. We find this to be indeed the case. When we ablate PVQR postembryonically (early L1 stage) in *zig-4 zig-3* double mutants, we observe that the flip-over of the axon of PVQL into the right VNC that usually occurs is completely suppressed (Figure 6C). These results corroborate previously conducted PVT/PVQR double ablation experiments (AURELIO *et al.* 2002). Unexpectedly, postembryonic ablation of either of two embryonically generated PVP neurons, whose axons closely fasciculate with the PVQ axons (see Figure 1 for schematic), also completely suppresses the PVQ axon flip-over defects of *zig-4 zig-3* mutants (Figure 6C). While the requirement of the PVP axon in the right cord (PVPL) may be similar to the requirement of the right PVQ axon (both may actively recruit and/or stabilize PVQL during/after a midline flip-over event), the suppression of the PVQL flip by ablating its directly neighboring left cord-residing PVPR axon is less obvious to explain. Apparently, if maintenance mechanisms are disabled, a latent activity of PVPR pushes the PVQL axon away into the opposite cord; eliminating PVPR removes this impetus and PVQL remains in the left fascicle.

DISCUSSION

We have identified a new maintenance factor, *zig-3*, which is required to stabilize axonal architecture at the ventral midline. We have identified the role of this factor in the course of a comprehensive mutant analysis of an entire family of small secreted Ig domain proteins. Most of them do not display a phenotype in the cellular context that we examined, but we surmise that they may have functions in other, as yet nonexamined cell types or that they may act in a redundant manner. A preliminary analysis of double mutant combinations indeed points to such a redundant scenario (C. BÉNARD and O. HOBERT, unpublished data). The only *zig* genes that display a phenotype on their own are the previously identified *zig-4* gene and the *zig-3* gene that we describe here.

The *zig-3* mutant phenotype corroborates key features of neuronal maintenance factors: (a) their absence causes no obvious developmental defects; (b) their activity is required during a critical period in the first larval stage; (c) they are not needed if locomotion of the animal is suppressed.

The function of *zig-3* appears intimately tied to that of the *zig-4* maintenance factor. Both genes are coexpressed by the same cell (the PVT neuron); their null

mutant phenotypes are indistinguishable and not mutually enhanceable. One possible interpretation of the linked nature of these two factors is that they act as heterodimers. A dimeric configuration has been observed for many other Ig domain proteins, particularly of the cell surface type in the immune system, historically the most intensively studied Ig domain proteins (BARCLAY *et al.* 1997). An obligate heterodimer model is also consistent with our observation that one protein cannot substitute for the other, even in an overexpression scenario. However, the function of ZIG-3 and ZIG-4 may not need to be as tightly molecularly linked; it is also possible that ZIG-3 and ZIG-4 affect one common pathway at distinct steps.

ZIG-3 and ZIG-4 may act as signaling proteins that activate receptor system(s). Alternatively, ZIG-3 and ZIG-4 may be part of a multimeric adhesion complex required to hold axons together in a fascicle. They may provide adhesive activity within such a complex or may alter the adhesive ability of other molecules.

The analysis of *zig-3* and *zig-4* mutants, as well as laser ablation studies, reveal a remarkable complexity of the mechanisms that hold the ventral nerve cord together. The pushing of axons through mechanical stress is clearly a necessary component for the induction of the flip-over event, as flip-overs (induced by loss of maintenance factors or PVT ablation) can be suppressed through immobilizing animals. However, mechanical force is clearly not sufficient to push axons around. First, vigorous movement of animals is already evident in the threefold embryo, yet axon flip-overs observed upon loss of PVT or maintenance factors only occur in the first larval stage. Second, movement does not result in flip-overs if the contralateral homolog of an axon is removed. One could argue that in such a case flip-over may in fact occur, but that a flipped axon requires its contralateral homolog to stabilize its position after it has flipped over the midline, perhaps via homophilic interaction. In the absence of such stabilization, a flipped axon may simply not remain in the opposite fascicle and be pushed back into its original fascicle. Such “pushing back” may occur passively by an increase in size of the midline structure (“hypodermal ridge”) occurring during larval stages. While an attractive model, the laser ablation of another class of ventral cord neurons, the PVP neurons complicates this model. The suppression of the left PVQ axon flip-over into the right fascicle also occurs when the PVP axon that is in the left ventral nerve cord is ablated. This cannot be a result of lack of stabilization of the flipped axons in the opposite cord, but rather suggests that the left cord PVP axon somehow provides a latent impetus for the left PVQ axon to move away into the opposite fascicle. Even though we find it hard to attach a molecular mechanism to these findings, the most conservative explanation is that there appears to be a tight balance of latent attractive and

repulsive events in the ventral nerve cord. Loss of PVT-mediated axon maintenance exposes axons to such latent attractive and repulsive forces, with axons being pushed and pulled over the midline. It will require the identification of more axon maintenance factors, and specifically a detailed analysis of their molecular interactions to more comprehensively understand these phenotypes.

We note that vertebrate nervous systems have to deal with similar challenges as the worm nervous system in that axon fascicles have to withstand mechanical stress from a variety of distinct sources (BÉNARD and HOBERT 2009). Moreover, a plethora of as yet uncharacterized small Ig domain proteins are expressed in the vertebrate brain as well (<http://www.brain-map.org/>) (BARCLAY *et al.* 1997). If some of those molecules are indeed involved in maintaining nervous system structure, they may be excellent candidates to be involved in neuronal pathologies, particularly adult-onset ones that may reflect a failure to maintain the specific architectural features of a nervous system.

We thank Q. Chen for expert technical assistance, the *Caenorhabditis* Genetics Center and particularly the *Caenorhabditis elegans* knockout consortia in Oklahoma, Vancouver, and Tokyo, under the leadership of R. Barstead, D. Moerman, and S. Mitani, respectively, for providing knockout strains; L. Segalat for providing the transposon insertion strain; and many colleagues in the worm community for providing reporter transgenes. This work was funded in part by the Muscular Dystrophy Association, the Boehringer Ingelheim Fond (to T.B.), the Natural Sciences and Engineering Research Council of Canada, and Canadian Institute of Health Research (to C.B.) and the Howard Hughes Medical Institute.

LITERATURE CITED

- AURELIO, O., D. H. HALL and O. HOBERT, 2002 Immunoglobulin-domain proteins required for maintenance of ventral nerve cord organization. *Science* **295**: 686–690.
- AURELIO, O., T. BOULIN and O. HOBERT, 2003 Identification of spatial and temporal cues that regulate postembryonic expression of axon maintenance factors in the *C. elegans* ventral nerve cord. *Development* **130**: 599–610.
- BARCLAY, A. N., M. H. BROWN, S. K. A. LAW, A. J. MCKNIGHT, M. G. TOMLINSON *et al.*, 1997 *The Leucocyte Antigen Facts Book*. Academic Press, London.
- BARGMANN, C. I., and L. AVERY, 1995 Laser killing of cells in *Caenorhabditis elegans*. *Methods Cell Biol.* **48**: 225–250.
- BÉNARD, C., and O. HOBERT, 2009 Looking beyond development: maintaining nervous system architecture. *Curr. Top. Dev. Biol.* **87**: 175–194.
- BÉNARD, C. Y., A. BOYANOV, D. H. HALL and O. HOBERT, 2006 DIG-1, a novel giant protein, non-autonomously mediates maintenance of nervous system architecture. *Development* **133**: 3329–3340.
- BRENNER, S., 1974 The genetics of *Caenorhabditis elegans*. *Genetics* **77**: 71–94.
- BŪLOW, H. E., T. BOULIN and O. HOBERT, 2004 Differential functions of the *C. elegans* FGF receptor in axon outgrowth and maintenance of axon position. *Neuron* **42**: 367–374.
- CLARK, S. G., and C. CHIU, 2003 *C. elegans* ZAG-1, a Zn-finger-homeodomain protein, regulates axonal development and neuronal differentiation. *Development* **130**: 3781–3794.
- FAY, D., and A. BENDER, 2008 SNPs: introduction and two-point mapping. *WormBook* September **25**: 1–10.
- GILLEARD, J. S., J. D. BARRY and I. L. JOHNSTONE, 1997 cis regulatory requirements for hypodermal cell-specific expression of the *Caenorhabditis elegans* cuticle collagen gene *dpy-7*. *Mol. Cell. Biol.* **17**: 2301–2311.
- HOBERT, O., 2002 PCR fusion-based approach to create reporter gene constructs for expression analysis in transgenic *C. elegans*. *Biotechniques* **32**: 728–730.
- HUTTER, H., 2003 Extracellular cues and pioneers act together to guide axons in the ventral cord of *C. elegans*. *Development* **130**: 5307–5318.
- JIN, Y., E. JORGENSEN, E. HARTWIEG and H. R. HORVITZ, 1999 The *Caenorhabditis elegans* gene *unc-25* encodes glutamic acid decarboxylase and is required for synaptic transmission but not synaptic development. *J. Neurosci.* **19**: 539–548.
- MCINTIRE, S. L., R. J. REIMER, K. SCHUSKE, R. H. EDWARDS and E. M. JORGENSEN, 1997 Identification and characterization of the vesicular GABA transporter. *Nature* **389**: 870–876.
- MUCH, J. W., D. J. SLADE, K. KLAMPERT, G. GARRIGA and B. WIGHTMAN, 2000 The *fax-1* nuclear hormone receptor regulates axon pathfinding and neurotransmitter expression. *Development* **127**: 703–712.
- NOTREDAME, C., D. G. HIGGINS and J. HERINGA, 2000 T-Coffee: a novel method for fast and accurate multiple sequence alignment. *J. Mol. Biol.* **302**: 205–217.
- OGURA, K., M. SHIRAKAWA, T. M. BARNES, S. HEKIMI and Y. OHSHIMA, 1997 The UNC-14 protein required for axonal elongation and guidance in *Caenorhabditis elegans* interacts with the serine/threonine kinase UNC-51. *Genes Dev.* **11**: 1801–1811.
- OKKEMA, P. G., S. W. HARRISON, V. PLUNGER, A. ARYANA and A. FIRE, 1993 Sequence requirements for myosin gene expression and regulation in *Caenorhabditis elegans*. *Genetics* **135**: 385–404.
- ORTIZ, C. O., J. F. ETCHBERGER, S. L. POSY, C. FROKJAER-JENSEN, S. LOCKERY *et al.*, 2006 Searching for neuronal left/right asymmetry: genomewide analysis of nematode receptor-type guanylyl cyclases. *Genetics* **173**: 131–149.
- POCOCK, R., C. Y. BÉNARD, L. SHAPIRO and O. HOBERT, 2008 Functional dissection of the *C. elegans* cell adhesion molecule SAX-7, a homologue of human L1. *Mol. Cell. Neurosci.* **37**: 56–68.
- ROUGON, G., and O. HOBERT, 2003 New insights into the diversity and function of neuronal immunoglobulin superfamily molecules. *Annu. Rev. Neurosci.* **26**: 207–238.
- SARAFI-REINACH, T. R., T. MELKMAN, O. HOBERT and P. SENGUPTA, 2001 The *lin-11* LIM homeobox gene specifies olfactory and chemosensory neuron fates in *C. elegans*. *Development* **128**: 3269–3281.
- SASAKURA, H., H. INADA, A. KUHARA, E. FUSAOKA, D. TAKEMOTO *et al.*, 2005 Maintenance of neuronal positions in organized ganglia by SAX-7, a *Caenorhabditis elegans* homologue of L1. *EMBO J.* **24**: 1477–1488.
- WANG, X., J. KWEON, S. LARSON and L. CHEN, 2005 A role for the *C. elegans* L1CAM homologue *lad-1/sax-7* in maintaining tissue attachment. *Dev. Biol.* **284**: 273–291.
- WHITE, J. G., E. SOUTHGATE, J. N. THOMSON and S. BRENNER, 1986 The structure of the nervous system of the nematode *Caenorhabditis elegans*. *Philos. Trans. R Soc. Lond. B Biol. Sci.* **314**: 1–340.
- ZALLEN, J. A., S. A. KIRCH and C. I. BARGMANN, 1999 Genes required for axon pathfinding and extension in the *C. elegans* nerve ring. *Development* **126**: 3679–3692.

Communicating editor: M. NONET

GENETICS

Supporting Information

<http://www.genetics.org/cgi/content/full/genetics.109.107441/DC1>

**The Small, Secreted Immunoglobulin Protein ZIG-3 Maintains
Axon Position in *Caenorhabditis elegans***

Claire Benard, Nartono Tjoe, Thomas Boulin, Janine Recio and Oliver Hobert

Copyright © 2009 by the Genetics Society of America

DOI: 10.1534/genetics.109.107441

FILE S1**SUPPORTING MATERIALS****Strains constructed and used in this work**

OH7375 *zig-1(ok81); oyIs14*
OH8833 *zig-1(ok81); oxIs12*
OH8835 *zig-1(ok81); hdIs26*
OH8910 *zig-1(ok81); zdIs13*
OH8895 *zig-1(ok81); bwIs2 otIs133*

OH7376 *zig-2(ok696); oyIs14*
OH8817 *zig-2(ok696); oxIs12*
OH8881 *zig-2(ok696); hdIs26*
OH8880 *zig-2(ok696); zdIs13*
OH8879 *zig-2(ok696); bwIs2 otIs133*

OH7019 *zig-3(tm924); oyIs14*
OH9113 *zig-3(gk33); oyIs14*
OH9012 *zig-3(tm924); juIs8*
OH9009 *zig-3(tm924); hdIs26*
OH9112 *zig-3(tm924); zdIs13*
OH7051 *zig-3(tm924); bwIs2 otIs133*

OH362 *zig-4(gk34); oyIs14*
OH8807 *zig-4(gk34); juIs8*
OH7394 *zig-4(gk34); hdIs26*
OH8877 *zig-4(gk34); zdIs13*
OH8610 *zig-4(gk34); bwIs2 otIs133*

OH8499 *zig-4(gk34) zig-3(tm924); oyIs14*
OH8498 *zig-4(gk34) zig-3(tm924); otIs173; oyIs14*
OH8813 *zig-4(gk34) zig-3(tm924); hdIs26*
OH8612 *zig-4(gk34) zig-3(tm924); zdIs13*
OH8758 *zig-4(gk34) zig-3(tm924); juIs8*
OH8609 *zig-4(gk34) zig-3(tm924); bwIs2 otIs133*

OH7378 *zig-5(ok1065); oyIs14*
OH7968 *zig-5(ok1065); oxIs12*
OH9013 *zig-5(ok1065); hdIs29*
OH9017 *zig-5(ok1065); zdIs13*
OH7970 *zig-5(ok1065); bwIs2 otIs133*

OH7379 *zig-6(ok723); oyIs14*
OH9009 *zig-6(ok723); juIs8*
OH8881 *zig-6(ok723); hdIs26*
OH8823 *zig-6(ok723); zdIs13*
OH8905 *zig-6(ok723); bwIs2 otIs133*

OH8185 *zig-7(ok2329); oyIs14*
OH9006 *zig-7(ok2329); oxIs12*
OH8894 *zig-7(ok2329); hdIs26*
OH9007 *zig-7(ok2329); zdIs13*
OH9010 *zig-7(ok2329); bwIs2 otIs133*

OH7380 *zig-8(ok561); oyIs14*
OH7975 *zig-8(ok561); oxIs12*
OH8876 *zig-8(ok561) hdIs26*
OH9173 *zig-8(ok561); zdIs13*

OH7977 *zig-8(ok561); bwIs2 otIs133*

OH9174 *egl-15(n484); otIs173; oyIs14*

OH8896 *sax-7(nj48); otIs173; oyIs14*

OH7592 *dig-1(hy188); otIs173; oyIs14*

OH9005 *zig-4(gk34) zig-3(tm924) egl-15(n484); otIs173; oyIs14*

OH9091 *sax-7(nj48); zig-4(gk34) zig-3(tm924); otIs173; oyIs14*

OH9001 *dig-1(hy188); zig-4(gk34) zig-3(tm924); otIs173; oyIs14*

DNA constructs and transgenic lines

All cloned PCR generated inserts were sequenced and were found to be fully wild type in sequence. While more transgenic lines were obtained in each case, we provide the names of 2 representative strains for each clone or construct injected.

4kb prom + *zig-3* genomic locus

The *zig-3* locus was PCR amplified using primers

oCB309 (F) aatatgattctcagattctcagacg

oCB310 (R) aagttaggggtacaattcaacagg

oCB307 (F*) agacatgAAGCTTtggttttcgggctagcgc

oCB308 (R*) atgcaaaaCCCGGGGgagcaaatgtttttggtggg

We injected this construct at 15 ng/ μ L, with 125 ng/ μ L of pRF4 into *zig-3(tm924); oyIs14*. We generated several lines among which:

OH9093 *zig-3(tm924); oyIs14; otEx4021*

OH9093 *zig-3(tm924); oyIs14; otEx4022*

Promoterless *zig-3* genomic PCR product

The *zig-3* locus was PCR amplified using primers

zNT1 atgctgctcatctgcatatc

oCB115 cattctgggttttcacaggg, and TA cloned the product.

We injected this clone at 15 ng/ μ L, with 125 ng/ μ L of pRF4 into *zig-3(tm924); oyIs14*. We generated several lines among which:

OH9122 *zig-3(tm924); oyIs14; otEx4043*

OH9123 *zig-3(tm924); oyIs14; otEx4044*

Short promoter *gfp* PCR fusion

zig-3 upstream regulatory sequence was PCR amplified using primers

zNT58 (A) gtcaataaacacattctcc

zNT26 (A*) tgtgaagtctctcaaaaacg

zNT59 (B) AGTCGACCTGCAGGCATGCAAGCTagcagcattttccaatgc

D* (HOBERT 2002).

We injected this PCR fusion at 15 ng/ μ L, with 125 ng/ μ L of pRF4 into N2. We generated several lines among which:

OH9175 +; *otEx4059*

OH9176 +; *otEx4060*

Short promoter PCR fusion for rescue assay

The *zig-3* locus was PCR amplified using primers

zNT26 tgtgaagtctctcaaaaacg

oCB115 cattctgggttttcacaggg

We injected this PCR product at 10 ng/ μ L, with 125 ng/ μ L of pRF4 into *zig-3(tm924); oyIs14* among which:

OH9120 *zig-3(tm924); oyIs14; otEx4041*

OH9121 *zig-3(tm924); oyIs14; otEx4042*

Pdpy-7::zig-3

The *zig-3* locus was PCR amplified using primers

oNT506 ttcaataaccgggATGCTGCTCATCTGCATATCTG

oNT507 ttcataccatggTTAAGCAATATGTTTTTGGTGGG

The PCR product was digested and ligated into *Pdpy-7* vector backbone at *XmaI-NcoI*.

We injected this clone at 10 ng/ μ L, with 125 ng/ μ L of pRF4 into *zig-3(tm924); oyIs14*. We generated several lines among which:

OH9097 *zig-3(tm924); oyIs14; otEx4025*

OH9098 *zig-3(tm924); oyIs14; otEx4026*

Punc-14::zig-3

The *zig-3* locus was PCR amplified using primers

oNT508 ttcatactagcATGCTGCTCATCTGCATATCTG

oNT507 ttcatactagcTTAAGCAATATGTTTTTTGGTGGG

The PCR product was digested and ligated into *Punc-14* vector backbone at sites *NheI-NcoI*.

We injected this clone at 15 ng/μL, with 125 ng/μL of pRF4 into *zig-3(tm924); oyIs14*. We generated several lines among which:

OH9099 *zig-3(tm924); oyIs14; otEx4027*

OH9100 *zig-3(tm924); oyIs14; otEx4028*

Pmyo-3::zig-3

The *zig-3* locus was PCR amplified using primers

oNT508 ttcatactagcATGCTGCTCATCTGCATATCTG

oNT507 ttcatactagcTTAAGCAATATGTTTTTTGGTGGG

The PCR product was digested and ligated into a *Pmyo-3* vector backbone at *NheI-NcoI*

We injected this clone at 30 ng/μL, with 125 ng/μL of pRF4 into *zig-3(tm924); oyIs14*. We generated several lines among which:

OH9101 *zig-3(tm924); oyIs14; otEx4029*

OH9102 *zig-3(tm924); oyIs14; otEx4030*

Pmyo-3::zig-3TM

We amplified the essential region the transmembrane domain of *pat-3* (*pat-3TM*) from pPD122.39 using primers

oCB255 catgctGGTACCGgataatgcaacagctcgggtc

oCB256 cagtctGGTACCTcggatctatcatgaag

and non-directionally inserted, in frame, this digested piece at the *KpnI* site upstream of *gfp* in pPD95.75, generating pCB115. We determined the correct orientation by restriction test digest and fully sequenced the insert.

We next inserted, in frame, a piece of *zig-3* locus upstream of the *pat-3TM* using primers oCB307 and oCB308, generating pCB144 *zig-3::pat-3TM*.

pCB144 served as a template to amplify a *zig-3::pat-3TM* fragment using primers:

oNT508 ttcatactagcATGCTGCTCATCTGCATATCTG

zNT47 tttccatggctacgggtacctcggatctatcatg

This PCR product was digested and ligated into *NheI-NcoI* sites of the *Pmyo-3::zig-3* vector from which the *zig-3* locus had been digested out.

We injected this *Pmyo-3::zig-3TM* clone at 30 ng/μL, with 125 ng/μL of pRF4 into *zig-3(tm924); oyIs14*. We generated several lines among which:

OH9132 *zig-3(tm924); oyIs14; otEx4053*

OH9133 *zig-3(tm924); oyIs14; otEx4054*

Pgcy-1::zig-3

We PCR amplified the *gcy-1* promoter using N2 genomic as template and primers

zNT45 ttttaagctgtgtactacaacaagggtctttg

zNT46 ttttgctagcgaatatttgcacgaaaag

We digested the PCR product and ligated it at sites *HindIII* and *NheI* to replace *Pmyo-3* in a *Pmyo-3* vector backbone.

We injected this clone at 20 ng/μL, with 125 ng/μL of pRF4 into *zig-3(tm924); oyIs14*. We generated several lines among which:

OH9124 *zig-3(tm924); oyIs14; otEx4045*

OH9125 *zig-3(tm924); oyIs14; otEx4046*

Pgcy-1::zig-3TM

We amplified the *gcy-1* promoter using N2 genomic as template, using primers:

zNT45 ttttaagctgtgtactacaacaagggtctttg

zNT46 ttttgctagcgaatatttgcacgaaaag

We inserted *Pgcy-1* at sites *HindIII* and *NheI* in *Pmyo-3::zig3::pat3TM*.

We injected this clone at 20 ng/μL, with 125 ng/μL of pRF4 into *zig-3(tm924); oyIs14*. We generated several lines among which:

OH9126 *zig-3(tm924); oyIs14; otEx4047*

OH9127 *zig-3(tm924); oyIs14; otEx4048*

Psra-6::zig-3

We PCR amplified the *sra-6* promoter using N2 genomic as template and primers:

zNT48 tttcagctgCCAACCTTTGTACAAAAAAGCAGGCTGGCAAAATCTGAAAT

AATAAATATTTAAATTC

zNT44 ttttgctagcCCAACCTTTGTACAAGAAAGCTGGGTCTTTTAGATATAATA

AATCGAAATTTGAAATG

We removed *Pmyo-3* in *Pmyo-3::zig-3* and replaced it by inserting *Psra-6* at sites *PvuII* and *NheI* of *Pmyo-3::zig-3*.

We injected this clone at 20 ng/μL, with 125 ng/μL of pRF4 into *zig-3(tm924); oyIs14*. We generated several lines among which:

OH9128 *zig-3(tm924); oyIs14; otEx4049*

OH9129 *zig-3(tm924); oyIs14; otEx4050*

Psva-6::zig-3TM

We used the same *Psva-6* as above (zNT48 and zNT44) to replace *Pmyo-3* in *Pmyo-3::zig-3::pat-3TM* and ligated it at sites *PvuII* and *NheI*.

We injected this clone at 20 ng/μL, with 125 ng/μL of pRF4 into *zig-3(tm924); oyls14*. We generated several lines among which:
 OH9130 *zig-3(tm924); oyls14; otEx4051*
 OH9131 *zig-3(tm924); oyls14; otEx4052*

Pmyo-3::zig-2

The *zig-2* locus was amplified from N2 template and cloned under the *myo-3* promoter of pPD95.86 at sites *NheI* and *NcoI*.

We injected this clone at 30 ng/μL, with 125 ng/μL of pRF4 into *zig-3(tm924); oyls14*. We generated several lines among which:
 OH9103 *zig-3(tm924); oyls14; otEx4031*
 OH9104 *zig-3(tm924); oyls14; otEx4032*

Pmyo-3::zig-4

The *zig-4* locus was amplified from N2 template and cloned under the *myo-3* promoter.

We injected this clone at 30 ng/μL, with 125 ng/μL of pRF4 into *zig-3(tm924); oyls14*. We generated several lines among which:
 OH9105 *zig-3(tm924); oyls14; otEx4033*
 OH9106 *zig-3(tm924); oyls14; otEx4034*

zig-4 genomic locus

We amplified the *zig-4* genomic locus using primers:

oCBona137 ccagtagtacggcagtcctc

oCBona138 cccgaaaattattgcgg

We injected this PCR product at 10 ng/μL, with 125 ng/μL of pRF4 into *zig-3(tm924); oyls14*. We generated several lines among which:

OH9095 *zig-3(tm924); oyls14; otEx4023*

OH9096 *zig-3(tm924); oyls14; otEx4024*

TABLE S1
Primers used for genotyping zig alleles

Allele	Primers to detect wild-type allele	Size of wild-type band	Primers to detect deletion allele	Size of mutant band
<i>zig-1</i> (<i>ok81</i>)	gcaggttgaatggtgccttttgacg gcgggaaaactcaactaataccctctg	328 bp	gcaggttgaatggtgccttttgacg cctctgctcagtaaaatgttcgtgag	691 bp
<i>zig-2</i> (<i>ok696</i>)	aaatatgctgaaatttaccgc ttatttagctagagtggtagagg	819 bp	ttgtcttgcaccacctaac agcaaagcaaagggcaacta	585 bp
<i>zig-3</i> (<i>tm924</i>)	gggtcctacagtcgagtcagg ccactggattttccggatgagaag	413 bp	aaaaatgctgctcatctgcatactgtcc ttaagcaatatgttttggggg	544 bp
<i>zig-3</i> (<i>gk33</i>)	cgaagtggaattctttacg tagctactgggatgatacc	458 bp	ctactccagtacaagaacc tagctactgggatgatacc	667 bp
<i>zig-4</i> (<i>gk34</i>)	atgtgatataatgccactcctgctgctacc cgcggttgggtaaaggaatgtttcttgccg	596 bp	ggccggttcaggagtacaacgacaacacag cgcggttgggtaaaggaatgtttcttgccg	924 bp
<i>zig-5</i> (<i>ok1065</i>)	aaaaatgtttcgtcctatccg ctcgaatatagttacatgtcaacc	468 bp	taccatgtttcgtcctatccg gcatgttcccgttatcgatttggcg	750 bp
<i>zig-6</i> (<i>ok723</i>)	cctagtctcttattcgtttgcagg cttgtgcttaccacctgaaacacc	675 bp	cctagtctcttattcgtttgcagg cgtttggtaaaatgttatcccattgtg	514 bp
<i>zig-7</i> (<i>ok2329</i>)	gaacgaaattcgcctgtgtcc tagatggaccagctatacc	659 bp	ttggttttagtcggacaccc gaacgaaattcgcctgtgtcc	526 bp
<i>zig-8</i> (<i>ok561</i>)	gtgtaggctaggaatcggtggg gcaagagcagataataggtagg	300 bp	aataagatcgctaaccgttataag gcaagagcagataataggtagg	337 bp